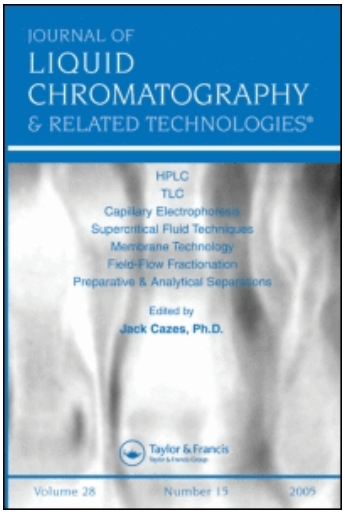

Journal of Liquid Chromatography & Related Technologies
Publication details, including instructions for authors and subscription information:
http://www.informaworld.com/smpp/title~content=t713597273

Effects of Molecular Weight and Flow Rate on Stress-Induced Migration of Polystyrene

Jianzhong Lou[a]; Vyas Harinath[a]
[a] Department of Mechanical and Chemical Engineering, North Carolina Agricultural and Technical State University, Greensboro, North Carolina, USA

Online publication date: 09 March 2004

To cite this Article Lou, Jianzhong and Harinath, Vyas(2005) 'Effects of Molecular Weight and Flow Rate on Stress-Induced Migration of Polystyrene', Journal of Liquid Chromatography & Related Technologies, 27: 18, 2819 — 2835
To link to this Article: DOI: 10.1081/JLC-200030476
URL: http://dx.doi.org/10.1081/JLC-200030476

JOURNAL OF LIQUID CHROMATOGRAPHY & RELATED TECHNOLOGIES®
Vol. 27, No. 18, pp. 2819–2835, 2004

Effects of Molecular Weight and Flow Rate on Stress-Induced Migration of Polystyrene

Jianzhong Lou* and Vyas Harinath

Department of Mechanical and Chemical Engineering, North Carolina Agricultural and Technical State University, Greensboro, North Carolina, USA

ABSTRACT

A simple scaling relation was proposed to predict the effects of molecular weight and flow rate on the stress-induced migration of polymer molecules subjected to simple shear flow. The predicted results were compared with experimental measurements in thermal field-flow fractionation (ThFFF). Retentions were measured for linear polystyrene samples with molecular weight up to thirty million. The experimental results were consistent qualitatively with the predictions.

Key Words: Polystyrene; Stress-induced migration; Field-flow fractionation.

*Correspondence: Professor Jianzhong Lou, Department of Mechanical and Chemical Engineering, North Carolina Agricultural and Technical State University, 1601 East Market St., Greensboro, NC 27411, USA; E-mail: lou@ncat.edu.

DOI: 10.1081/JLC-200030476 1082-6076 (Print); 1520-572X (Online)

INTRODUCTION

Separation of polymers for molecular weight analysis is routinely done using gel-permeation chromatography (GPC) in most industrial laboratories. However, pore size upper limit, mechanical degradation, sample adsorption, and low selectivity often become issues for many polymer samples, especially in the high molecular weight range. The problems are often associated with the porous gel particles in the GPC column. Two competing technologies, the hydrodynamic chromatography (HDC) and the thermal field-flow fractionation (ThFFF), with columns (or channels) that are not packed with porous particles, offer promising alternatives to the analytical separation of many polymers. The separation of polymers in both HDC and ThFFF is achieved by mechanisms that locate the polymer molecules to the different cross-sectional positions across the non-uniform velocity profile of the flow of the solvent (mobile phase or the carrier), and the polymer molecules are swept out of the channel by the solvent at different velocities. In a capillary hydrodynamic chromatography (CHDC) column, the polymer molecules are excluded from the wall region of the column where velocity is the lowest.[1] Therefore, the average velocity of the polymer molecules is faster than that of the solvent, with higher velocity for the polymer molecules of larger hydrodynamic radius than the polymer molecules of smaller hydrodynamic radius. Non-porous particles are often used to pack the capillary column to create more effective micro-capillaries, which exist in the inter-particle spaces in so-called packed-column hydrodynamic chromatography (PHDC).[2] In the ThFFF channel, an externally applied thermal field force drives the polymer molecules to an equilibrium distribution near the accumulation wall.[3] The polymer molecules of larger diffusion coefficient spread out more from the accumulation wall than the polymer molecules of lower diffusion coefficient, and elute through the ThFFF channel at high average velocity. One issue, which remains little understood but is of fundamental importance for understanding the mechanisms of the separation in both ThFFF and HDC methods, is the so-called stress-induced polymer migration that contributes to the so-called lift forces driving the polymer molecules laterally across the shear flow laminae.[4] In order to develop the separation techniques, it is desirable to understand the molecular weight and shear rate (or flow rate) dependence of the stress-induced migration or the lift forces in simple shear flow.

The stress-induced polymer migration was discovered as early as 1965 in polyethylene melt extrusion, when difference in molecular weight was noticed between the surface and the center of the extrudates.[5] It was not until the migration of polymer chains in a solvent under shear flow was first reported in Ref.[6], that the great potential it represented for separation and chromatography was recognized. Dill and Zimm proposed the cone-shaped shear flow

geometry for DNA separation based on the radial migration towards the center of the cone.[7] Cohen et al. measured the apparent viscosity for aqueous solutions of polyacrylamide in capillary flow, and attributed the decrease in the apparent viscosity of the polymer solution to the migration of polymer molecules away from the wall region, and thus causing an apparent slip on the wall.[8,9] Gao et al. used the so-called lift forces in hyperlayer-mode ThFFF to separate polystyrenes of ultrahigh molecular weight.[10] Sugarman measured the radial migration of polyacrylamide and DNA molecules in aqueous solutions using CHDC.[11]

Cox and Brenner established the theory for lift forces of an inertial origin for solid particles in Poiseuille flow.[12] Williams et al. demonstrated the existence of near-wall lift forces and characterized their dependence on particle size and shear rate in separation of particles in the sedimentation field-flow fractionation (FFF) channel.[13–15] In comparison, the molecular-level lift forces responsible for stress-induced polymer migration in ThFFF and CHDC appear to be much less understood and probably involve somewhat more complicated origins than particles. Polymer chains become deformed in the flow. Understanding this deformation process is an essential part of polymer reology research because the polymer chains are ultimately responsible for the viscoelastic flow properties of a polymeric fluid being solutions or melts. Despite this obvious importance, there has been little effort to characterize stress-induced lift forces on polymer chains in ThFFF or HDC. Several rather complex physical models were created to predict the stress-induced polymer migration in both non-curvature and curvature flow geometries, such as the kinetic theory[16–18] and the non-equilibrium thermodynamics models.[19–22] These models predict rather different concentration profiles of polymers in various flow conditions and geometries. None of them has been validated with ThFFF or HDC experimental data. For example, the model created by Tirrell and Malone[4] predicts a chemical potential:

$$\mu = kT\left(\frac{1}{3}\lambda^2\dot{\gamma}^2 - \frac{1}{2}\ln\left(1 + \frac{2\lambda^2\dot{\gamma}^2}{3}\right)\right) \tag{1}$$

where μ is the chemical potential, k is the Boltzmann constant, T is the absolute temperature, λ is the relaxation time, $\dot{\gamma}$ is the shear rate, and the product $\lambda\dot{\gamma}$ is known as the Deborah number, which is a measure of shear deformation or the ratio of the shear energy to the thermal energy. Sugarman's experiments on the CHDC showed that the predicted dependence on the Deborah number was incorrect.[11] Other models made predictions, although not in agreement with one another, in rather complicated numerical and implicit ways that are not readily useful in predicting the retention behavior in ThFFF and HDC of polymers.[19–22]

The objective of this paper is to develop a simple scaling relation for the dependence of the stress-induced polymer migration on the molecular weight and the flow rate, and then compare the results with hyperlayer ThFFF measurement using polystyrene samples. The results should provide further insights needed for the development of the separation technique.

SCALING THEORY

We shall propose that the lift forces are the gradient of the elastic energy associated with the reversible shear deformation of polymer chains in simple shear flow. The elastic energy relates to the energy required in the recoiling process of the shear-deformed polymer chains. Among the quantities that are most relevant to the elastic energy in shear flows of polymeric fluid, is the first normal stress difference N_1, which is defined as,

$$N_1 = \psi_1 \dot{\gamma}^2 \tag{2}$$

where ψ_1 is the first normal stress difference coefficient, $\dot{\gamma}$ is the shear rate. From dimensional analysis, this quantity N_1 is proportional to the elastic energy in unit volume of the fluid. We can argue that the elastic energy is proportional to N_1. The first normal stress difference coefficient is a basic material function of a polymeric liquid. In the dilute solution theories, the first normal stress difference coefficient is related to Zimm's longest relaxation time λ and the viscosity η (approximately equal to the solvent viscosity η_0 for dilute solutions) by the Odroyd-B equation:

$$\psi_1 = 2\lambda\eta_0 \tag{3}$$

The relaxation time λ in the Zimm theory for dominant hydrodynamic interactions[23] is:

$$\lambda = \frac{6[\eta]\eta_0 M}{1.44\pi^2 RT} \tag{4}$$

where $[\eta]$ is the intrinsic viscosity, η_0 the solvent viscosity, M the polymer molecular weight, and R the gas constant. The elastic energy is, therefore, related to:

$$\varepsilon_{\text{elastic}} \propto \eta_0^2[\eta]M\dot{\gamma}^2 \tag{5}$$

In a good solvent, as typical in polymer separation in ThFFF and HDC, the intrinsic viscosity for a linear polymer is approximately proportional to the 4/5th power of the molecular weight.[24,25] Therefore,

$$\varepsilon_{\text{elastic}} \propto \eta_0^2 M^{9/5}\dot{\gamma}^2 \tag{6}$$

The lift forces can be formulated as the gradient of the elastic energy, with the negative sign to signify that the lift forces migrate polymer chains towards lower elastic energy region across the flow:

$$F_L \propto -\frac{d\varepsilon_{\text{elastic}}}{dy} \propto -\eta_0^2 M^{9/5} \dot{\gamma} \frac{d\dot{\gamma}}{dy} \tag{7}$$

where y is the coordinate perpendicular to the velocity of the flow. For the isothermal parallel-plate Poiseuille flow, the shear rate and shear rate gradient are calculated from the velocity profile:

$$u(y) = 6\langle u \rangle \left(\frac{y}{w} - \frac{y^2}{w^2} \right) \tag{8}$$

$$\dot{\gamma}(y) = \frac{6\langle u \rangle}{w} \left(1 - \frac{2y}{w} \right) \tag{9}$$

$$\frac{d\dot{\gamma}}{dy} = -\frac{12\langle u \rangle}{w^2} \tag{10}$$

where, $u(y)$ is the velocity profile across the flow, y in parallel-plate Poiseuille flow is the elevation from one of the channel walls (the accumulation wall for the ThFFF channel), w is the distance between the two parallel channel walls, $\langle u \rangle$ is the average velocity of the flow in the channel. Finally, the lift forces in isothermal parallel-plate Poiseuille flow (applicable to ThFFF with slight departure due to existence of a temperature gradient) will be proportional to:

$$F_L \propto \eta_0^2 M^{9/5} \langle u \rangle^2 \tag{11}$$

For Poiseuille flow in a circular tube, as in the CHDC column, the result will be slightly different due to the velocity profile:

$$u(r) = 2\langle u \rangle \left(1 - \frac{r^2}{R^2} \right) \tag{12}$$

$$\dot{\gamma}(r) = \frac{4\langle u \rangle r}{R^2} \tag{13}$$

$$\frac{d\dot{\gamma}}{dr} = \frac{4\langle u \rangle}{R^2} \tag{14}$$

where $u(r)$ is the velocity profile across the flow, r is the radial coordinate; R is the radius of the flow column. However, the molecular weight and shear (or flow) dependence, which resulted from the above argument will be the same as in (ThFFF) parallel-plate Poiseuille flow.

In the so-called hyperlayer-mode of FFF, an externally applied field force drives the particles or polymer molecules to the accumulation wall, and the opposing lift forces push the particles or polymer molecules away from

the accumulation wall. The combined result of the lift forces and the applied external field force is that the particles or the polymer molecules are forced into thin layers of different equilibrium elevations (designated as y_{eq}) away from the accumulation wall (at the wall, $y = 0$). Since the flow velocity of the carrier in the FFF channel (parallel-plate laminar flow) is dependent upon the elevation above the accumulation wall, the polymer molecules are swept out at different velocities and are separated. This has been clearly illustrated by Giddings who developed the FFF family of analytical separation techniques.[3] Giddings predicted that the polymer concentration profile in the hyperlayer-mode thermal FFF is a Gaussian distribution centered at equilibrium elevation y_{eq}.[26,27] The temperature profile in thermal FFF makes the viscosity and velocity profile slightly different from that in the isothermal flow system. In a recent study of lift forces on polystyrene particles subjected to sedimentation FFF, Williams et al.[28] calculated the values of the lift forces by simply assuming that at the point of equilibrium, the field force exerted on the particle will exactly counter the lift forces:

$$F_L = F_{\text{field}} \tag{15}$$

Since the sample particles are also subject to concentration-induced diffusion force, such an approach appears to be good for the ideal case where the diffusion force is neglected compared with the field force and the lift forces.

Williams et al. recommended two strategies to deal with the sample relaxation to its equilibrium position caused by the flow-induced lift forces.[28] The first one was to stop the flow after introducing the sample to the FFF channel to allow the sample to be driven by the field force to close to the accumulation wall, and when the flow is restored, the relaxation by the lift forces will be minimal because the sample is already close to its equilibrium position. This method was used to measure lift forces using FFF data.[13,14] The second method, recommended by Williams et al., involved the estimation of the distance the sample traveled during relaxation.[28] However, as we will show below, even for polystyrene samples of molecular weight below one million dalton, completely neglecting the lift force would introduce errors at relatively high flow rates. At the same time, even at high flow rate and for higher molecular weight polystyrene samples, when lift forces are expected to dominate, completely neglecting the diffusion force will lead to errors.

The theory of the thermal field force was well established by Giddings and coworkers.[3,29,30] For given experimental conditions, the thermal field force is a function of thermal diffusion coefficient D_T

$$F_{\text{field}} = -\frac{kTD_T}{D}\left(\frac{dT}{dy}\right) \tag{16}$$

where k is the Boltzmann constant, T is absolute temperature, D is diffusion coefficient, (dT/dy) is the temperature gradient (approximately equal to temperature drop ΔT divided by the channel thickness w). The negative sign stands for the direction of the field force being opposite to the temperature gradient. The thermal diffusion coefficient, D_T, is essentially independent of molecular weight for a given polymer type, which was shown by experimental data.[29] The calibration curve for thermal FFF in normal mode provides the molecular weight dependence of the thermal field force through (D/D_T):[29,30]

$$\frac{D}{D_T} = \phi M^{-n} \tag{17}$$

where ϕ and $(-n)$ are the intercept and slope in the $\log(D/D_T)$ vs. $\log M$ plot, respectively. For a given polymer type and solvent, the thermal field force is calculated from the temperature drop ΔT and molecular weight:

$$F_{Th} = K_{Th} M^n \Delta T \tag{18}$$

where K_{Th} and n are constants for a given polymer type, solvent, and temperature. We assume the lift forces depend on both molecular weight and shear rate $\dot{\gamma}$ for a given polymer type, solvent, and temperature. The shear rate $\dot{\gamma}$ in the FFF channel is a function of the elevation y [as in Eq. (9), w is the thickness of the FFF channel, $\langle u \rangle$ is the average velocity of the flow in the channel]. For a given elevation y, the shear rate $\dot{\gamma}$ is proportional to the flow rate Q or the average velocity $\langle u \rangle$. Inspired by the power law empirical correlation developed by Williams et al.,[13,14] and the scaling relation we proposed earlier, we shall assume that the molecular weight and flow rate dependence of the lift forces takes in the following form at a given elevation:

$$F_L = K_L M^a \langle u \rangle^b \tag{19}$$

where K_L, a, and b are another set of constants for a given polymer type, solvent, and temperature to be experimentally determined. The exponent b reflects the shear rate influence on the lift forces, but can be determined from hyperlayer-mode thermal FFF data of varying flow rate for a given elevation. In the hyperlayer-mode thermal FFF, the lift forces must be equal to the applied thermal field force, resulting in the following equation:

$$M^{(a-n)} = \frac{K_{th}}{K_L} \Delta T \langle u \rangle^{-b} \tag{20}$$

A more convenient equation is the following log–log form:

$$\log M = \frac{1}{a-n}\log \Delta T - \frac{b}{a-n}\log \langle u \rangle + \frac{1}{a-n}\log\left(\frac{K_{\text{th}}}{K_{\text{L}}}\right) \tag{21}$$

Using the assumption [Eq. (15)] made by Williams et al.[28] and the stop-flow strategy recommended by Williams et al.,[28] we can plot thermal FFF retention data of hyperlayer-mode in the form of $\log M$ vs. $\log \Delta T$ at constant flow rate Q (or average velocity $\langle u \rangle$), and $\log M$ vs. $\log Q$ at constant temperature drop ΔT, for any given equilibrium elevation y_{eq} or retention ratio t^0/t_{r}, (t^0 is the elution time of the solvent peak, t_{r} is the retention time of the polymer peak). We can then determine the values for a and b for lift forces. Note that the n value is calculated from the normal mode thermal FFF calibration curve, as detailed in the FFF literature.[3,26–30]

EXPERIMENTAL

The thermal FFF system used in this work was of conventional design. The surfaces of the two copper bars enclosing the channel were chrome plated and finely polished. Four 1-kW cartridge heaters were inserted into the hot bar. Passages were drilled into the cold bar to allow tap water to run through as a coolant. The temperature drop was controlled precisely between the bars by computer. Both a 50- and a 76-μm thick Mylar polyester spacers were clamped tightly between the bars by 22 evenly spaced bolts. The center of the spacer was cut out to leave a ribbon-like flow channel measuring 2 cm in breadth and 47.3 cm in tip-to-tip length.

A Spectra-Physics (San Jose, CA) Isotherm LC pump was used to deliver chromatography-grade tetrahydrofuran (THF) solvent to a Rheodyne (Sotati, CA) sample injector, which was connected to the inlet of the thermal FFF channel. The injection loop was 10-μL, and Hamilton (Reno, NV) Microlite injection syringes of 2.5 and 10 μL capacities were used for sample injection. The dead volume between the channel and the injector was measured to be 25 μL. The stop-flow period (to allow the polymer sample to relax under thermal field force) used was 18–30 sec. A Rheodyne auto-injection valve (Model 5701) was used to operate the post-injection delay and the stop flow with computer control. An Applied Biosystems (Foster City, CA) Model 757 UV detector was used with the wavelength set at 260 nm for polystyrenes.

Linear polystyrene standards covering a wide molecular weight range were used in this study. They are listed in Table 1. Chromatography-grade THF was used for sample preparation. Polystyrenes were dissolved in room

Table 1. Polystyrene samples.

Sample ID #	Molecular weight	Polydispersity	Vendor
1	400,000	1.06	Pressure chemical
2	498,000	1.2	Pressure chemical
3	900,000	1.06	Pressure chemical
4	1,970,000	1.1	American polymer
5	2,860,000	1.09	American polymer
6	4,480,000	1.14	American polymer
7	5,480,000	1.15	American polymer
8	6,770,000	1.14	American polymer
9	8,420,000	1.17	American polymer
10	10,000,000	n.a.	Polysciences
11	20,000,000	1.2	Pressure chemical
12	30,000,000	1.3	Polysciences

Note: n.a., Not available.

temperature. The final concentration of the solutions for injection to the FFF channel was adjusted to 0.01–0.1% (w/v).

RESULTS AND DISCUSSION

At flow rates below 1.2 mL/min, the experimental results showed the normal mode retention sequence: the retention time t_r of higher molecular weight samples was longer (the retention ratio, t^0/t_r, was smaller). This was expected for normal mode thermal FFF, because the higher molecular weight polymer chains were less likely to diffuse away from the accumulation wall when they were pushed to the accumulation wall by the thermal field force. As described above, normal-mode thermal FFF runs were needed for determining the constant $(-n)$. The slope of the molecular weight calibration curve was calculated from normal mode thermal FFF retention data to be -0.591 (with standard error of 0.06 with five molecular weight samples, two flow rates, two duplicates, total of 20 data points) and, therefore, $n = 0.591$. When the flow rate was increased, the sequence of retention was changing at molecular weight around two million, indicating the lift forces became significant relative to the thermal field force. Eventually, the sequence of the retention became hyperlayer-mode where the higher molecular weight sample eluted before lower molecular weight samples. This meant that in the hyperlayer-mode, higher molecular weight polymer molecules migrated by the lift forces to higher equilibrium elevations (y_{eq}) where the velocity was

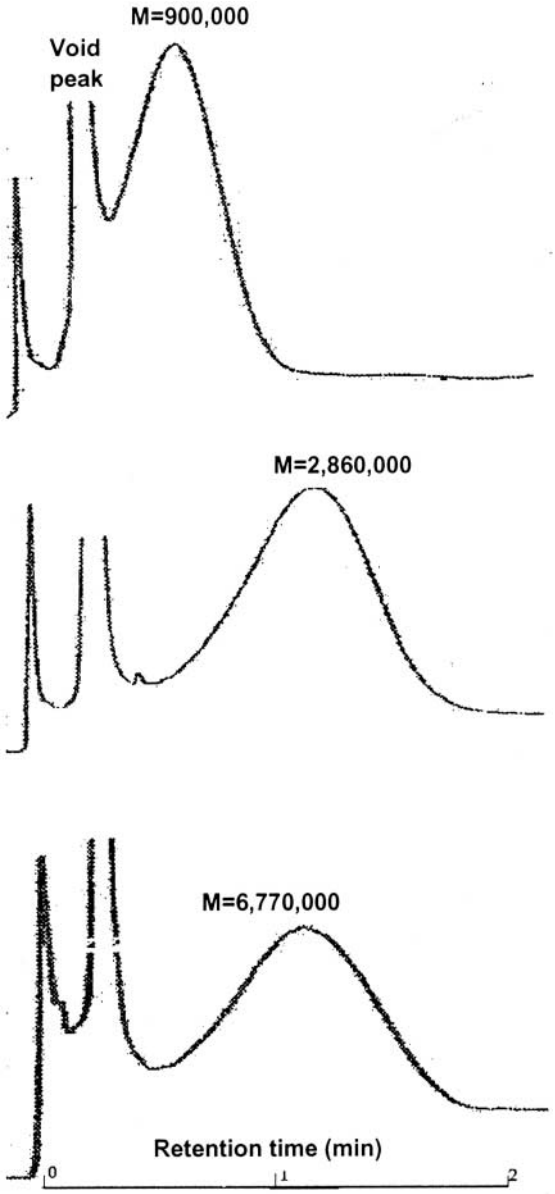

Figure 1. Typical thermal FFF fractograms showing the effect of the lift forces and the transition of retention sequence for different molecular weight polystyrene samples. The experimental conditions were: temperature drop was 20°C, cold wall temperature was 30°C, channel flow rate at 1.8 mL/min.

higher. The transition from normal mode to hyperlayer-mode was facilitated by increases in both molecular weight M and flow rate Q as expected. Typical experimental data are illustrated in Fig. 1 where constant flow rate was used for different molecular weight samples. It was evident that the retention time first increased as the molecular weight increased, but started to decrease as the molecular weight increased further.

In Fig. 2, the transition from normal mode to hyperlayer-mode was shown with respect to the changes in molecular weight at several field strengths in terms of ΔT. In Fig. 3, the applied thermal field was fixed and the flow rate was varied, which also affected the transition.

As shown in Figs. 2 and 3, at the inversion point the maximum retention times or minimum retention ratios were reached. Correspondingly, the retention selectivity of the molecular weight was totally lost at the inversion point. If the inversion point exists, then no polymer samples should elute after the maximum retention time. This also means that two different molecular weight samples should co-elute at the same retention time, one being retained according to the normal mode mechanism and the other according to the hyperlayer-mode mechanism. The experimental elution data did not show a clear inversion point, rather, a relatively wide transition region (instead of a

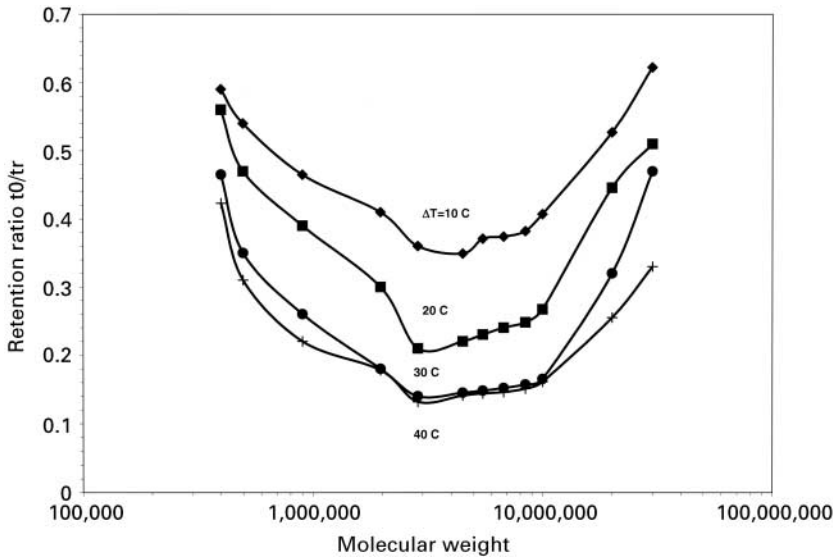

Figure 2. Typical retention ratio t^0/t_r data as a function of molecular weight M of the polystyrene samples at several temperature drops ΔT (°C). The experimental conditions were: cold wall temperature was 30°C, channel flow rate at 2.0 mL/min.

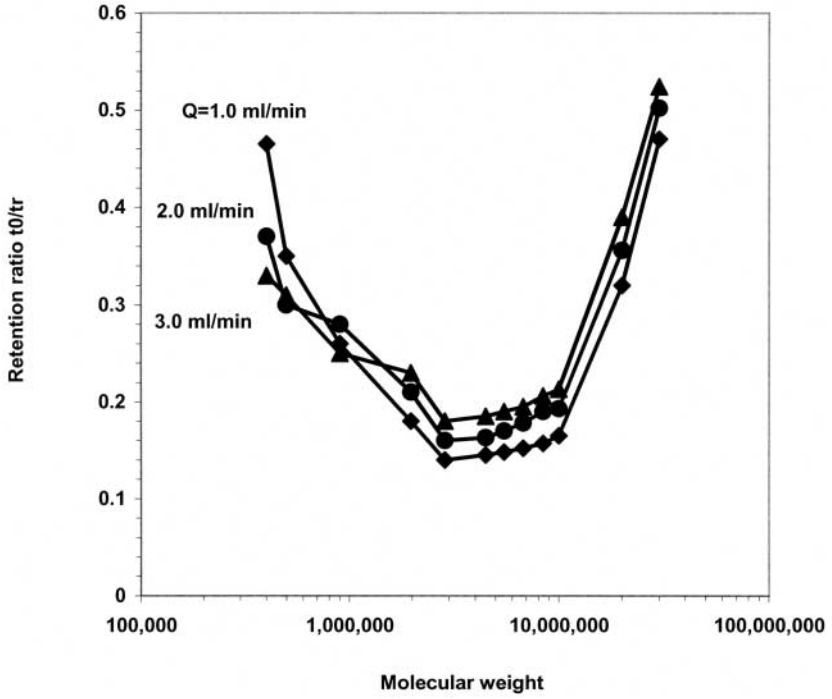

Figure 3. Typical retention ratio t^0/t_r data as a function of molecular weight M of the polystyrene samples at several channel flow rates Q (mL/min). The experimental conditions were: temperature drop was 30°C, cold wall temperature was 30°C.

point) was observed over the molecular weight range from two million to about ten million dalton. The thermal FFF experiment at high flow rates was very fast (in a few minutes) and this allowed numerous repeat runs in order to track the inversion point. The observed transition is the result of balance between two mechanisms (or modes): the normal mode where the diffusional force is important and the hyperlayer-mode where the lift forces are dominant. The difficulty in calculating lift forces from the experimental data using the assumption made by Williams et al. [Eq. (15)],[28] is apparent due to the coexistence of both lift forces and the diffusional force in these experiments. It would be highly desirable for one to neglect the diffusion force, using "pure" hyperlayer-mode experimental data to calculate the lift forces using the assumption by Williams et al. [Eq. (15)].[28]

Polystyrenes are the most widely used narrow molecular weight standards and the available polystyrene samples cover the broadest range of molecular weight.

It was shown in Fig. 3, that with the increase in flow rate, the retention time decreased. This was consistent with the understanding that the lift forces that moved the polymer molecules away from the accumulation wall increased with flow rate. In contrast, Fig. 2 showed that the increase in the temperature drop ΔT actually increased the retention time of the polymer samples. In other words, the stronger the field force that pushed the polymer molecules, the closer the sample was to the accumulation wall where the velocity was lower and the lift forces were weaker.

As a result of the difficulty in applying the assumption made by Williams et al.,[28] we had to choose to identify the onset of the "pure" hyperlayer-mode. By approximation, this onset was determined so that only hyperlayer-mode retention data were used to calculate the lift. The parameter n was substituted by 0.591 from normal mode calibration data:

$$\log M = \frac{1}{a - 0.591} \log \Delta T - \frac{b}{a - 0.591} \log \langle u \rangle + \frac{1}{a - 0.591} \log\left(\frac{K_{\text{th}}}{K_{\text{L}}}\right) \tag{22}$$

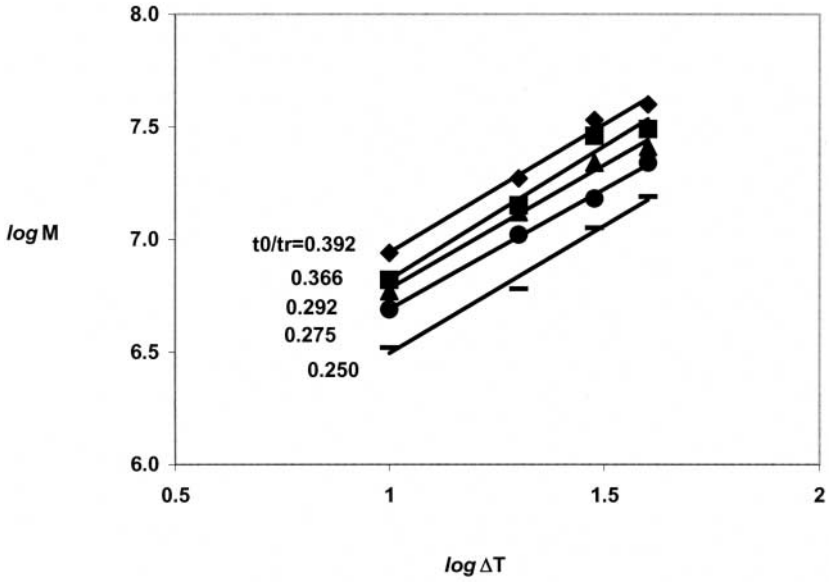

Figure 4. Retention data plotted in the form of $\log M$ vs. $\log \Delta T$ [see Eq. (22)] for evaluating the molecular weight M dependence of the lift forces at several retention ratios t^0/t_{r}.

Figure 4 is such a plot of $\log M$ vs. $\log \Delta T$. The data points were obtained from interpolation at constant retention ratio or equilibrium elevation from the approximately "pure" hyperlayer-mode retention data. In the process, the flow rate was fixed so only the temperature drop varied. This was done for several retention ratio values. The slopes from the plot were scattered but still an average value for the slope was obtained with an error of less than 11%:

$$\text{Average}\left(\frac{1}{a-0.591}\right) = 1.12 \tag{23}$$

From this average slope, we then obtained the a value to be 1.48.

Figure 5 is a plot of $\log M$ vs. $\log Q$ (Q is the channel flow rate in mL/min and is proportional to average velocity for a given FFF channel) for several retention ratios in hyperlayer-mode. The average slope was 0.94 and we calculated the b to be 0.84.

It should be clearly noted that the estimated lift force effects from the hyperlayer-mode experimental data are only to the best a qualitative check on our proposed scaling theory. The requirement to satisfy the assumption

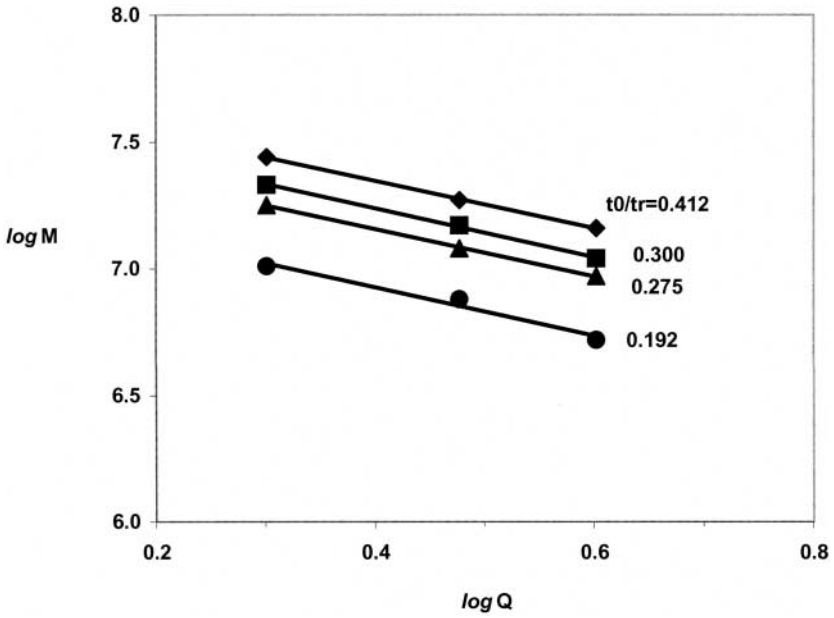

Figure 5. Retention data plotted in the form of $\log M$ vs. $\log Q$ [see Eq. (22)] for evaluating the flow rate Q dependence of the lift forces at several retention ratios t^0/t_r.

made by Williams et al. [Eq. (15)][28] is that in such estimate of lift forces, the diffusion force must be completely neglected and as we have shown here, such experimental conditions are hard to attain. The experimental data also showed the dependence of the dimensionless retention ratio on the flow rate for the data in the normal mode. This actually means that at the flow rates we were running, even the relatively low molecular weight samples were subjected to the lift forces that were the reason for flow rate dependence. Further research is clearly indicated in this area.

CONCLUSIONS

We formulated a simple relation to predict the molecular weight and flow (shear) dependence for the lift forces caused by polymer deformation in simple shear flows. The argument was hypothetic. It predicts the lift forces dependent on the 2nd power of both flow rate (or average velocity) and the viscosity and on the 9/5th power of the polymer molecular weight.

The hyperlayer transition in thermal FFF for polystyrene samples was a gradual process that covered a relatively wide region of molecular weight from about two million to ten million. This made the lift force measurement relatively difficult, due to the limit on available polymer samples that will be completely eluted in thermal FFF in the pure hyperlayer-mode mechanism. Using the assumption and the stop flow procedure as recommended in the literature,[28] we made qualitative check on the lift forces with hyperlayer-mode FFF experimental data, and found that the lift forces depend on 1.48th power of molecular weight. The experimental fit of flow rate dependence of lift force was relatively poor. The trend appears to be consistent with our scaling theory with a considerable amount of discrepancy. This scaling theory and the qualitative support of the experiments are meaningful, in that no prior such study has been reported to show such an agreement between the theory and the experiments. Further work is clearly indicated, and this study should help promote more research efforts on the subject.

REFERENCES

1. Orr, C.; Mullins, M.E. Capillary hydrodynamic chromatography. J. Chromatogr. A **1978**, *166* (2), 373–382.
2. Stegeman, G.; Kraak, J.C.; Poppe, H.; Tijssen, R. Hydrodynamic chromatography of polymers in packed columns. J. Chromatogr. A **1993**, *657* (2), 283–303.
3. Giddings, J.C. Field-flow fractionation: analysis of macromolecular, colloidal, and particulate materials. Science **1993**, *260*, 1456–1465.

4. Tirrell, M.; Malone, M.F. Stress-induced diffusion of macromolecules. J. Polym. Sci. Polym. Phys. **1977**, *15* (9), 1569–1583.
5. Schreiber, H.P.; Storey, S.H. Molecular fractionation in capillary flow of polymer fluids. J. Polym. Sci. Polym. Lett. **1965**, *3* (9), 723–731.
6. Shafer, R.H.; Laiken, N.; Zimm, B.H. Radial migration of DNA molecules in cylindrical flow. I. Theory of the free-draining model. Biophys. Chem. **1974**, *2* (2), 180–184.
7. Dill, K.A.; Zimm, B.H. A rheological separator for very large DNA molecules. Nucleic Acids Res. **1979**, *7* (3), 735–749.
8. Metzner, A.B.; Cohen, Y.; Rangel-Nafaile, C. Inhomogenous flows of non-Newtonian fluids: generation of spatial concentration gradients. J. Non-Newtonian Fluid Mech. **1979**, *5*, 449–462.
9. Cohen, Y.; Metzner, A.B. An analysis of apparent slip flow of polymer solutions. Rheol. Acta **1986**, *25* (1), 28–35.
10. Gao, Y.S.; Caldwell, K.D.; Myers, M.N.; Giddings, J.C. Extension of thermal field-flow fractionation to ultra-high molecular weight polystyrenes. Macromolecules **1985**, *18* (6), 1272–1277.
11. Sugarman, J.H.. Microcapillary Chromatography and Radical Migration of Water-Soluble Polymers. Princeton University, 1988; Ph.D. Thesis.
12. Cox, R.G.; Brenner, H. The lateral migration of solid particles in Poiseuille flow. I. Theory. Chem. Eng. Sci. **1968**, *I*, 147–173.
13. Williams, P.S.; Koch, T.; Giddings, J.C. Characterization of near-wall hydrodynamic lift forces using sedimentation field-flow fractionation. Chem. Eng. Commun. **1992**, *111*, 121–147.
14. Williams, P.S.; Moon, M.H.; Giddings, J.C. Fast separation and characterization of micron size particles by sedimentation/steric field-flow fractionation: role of lift forces. In *Particle Size Analysis*; Stanley-Wood, N.G., Lines, R.W., Eds.; Royal Society of Chemistry: Cambridge, UK, 1992; 280–289.
15. Williams, P.S.; Lee, S.; Giddings, J.C. Characterization of hydrodynamic lift forces by field-flow fractionation: inertial and near-wall lift forces. Chem. Eng. Commun. **1994**, *130*, 143–166.
16. Aubert, J.H.; Tirrell, M. Macromolecules in non-homogenous velocity gradient field. J. Chem. Phys. **1980**, *72*, 2694–2701.
17. Aubert, J.H.; Prager, S.; Tirrell, M. Macromolecules in non-homogenous velocity gradient field. Part II. J. Chem. Phys. **1980**, *73*, 4103–4112.
18. Aubert, J.H.; Tirrell, M. Effective viscosity of dilute polymer solutions near confining boundaries. J. Chem. Phys. **1982**, *77*, 553–561.
19. del Castillo, L.F.; Criado-Sancho, M.; Jou, D. Nonequilibrium chemical potential and shear-inducing migration of polymers in dilute solutions. Polymer **2000**, *41*, 2633–2638.

20. Jou, D.; Criado-Sancho, M.; Casas-Vazquez, J. Non-equilibrium chemical potential and stress-induced migration of polymers in tubes. Polymer **2002**, *43* (5), 1599–1605.
21. Beris, A.N.; Mavrantzas, V.G. On the compatibility between various macroscopic formalisms for the concentration and flow of dilute polymer solutions. J. Rheol. **1994**, *38*, 1237–1250.
22. Mavrantzas, V.G. Surface Effects on the Comformation and Rheology of Dilute Polymer Solutions. University of Delaware, 1994; Ph.D. Thesis.
23. Zimm, B.H. Dynamics of polymer molecules in dilute solution: viscoelasticity, flow birefringence, and dielectric loss. J. Chem. Phys. **1956**, *24*, 269–278.
24. de Gennes, P.-G. *Scaling Concepts in Polymer Physics*; Cornell University Press: Ithaca, NY, 1979.
25. Larson, R.G. *Constitutive Equations for Polymer Melts and Solutions*; Butterworths: Boston, MA, 1988.
26. Giddings, J.C. Hyperlayer field-flow fractionation. Sep. Sci. Technol. **1983**, *18* (8), 765–773.
27. Giddings, J.C. *Unified Separation Science*; Wiley: New York, 1991.
28. Williams, P.S.; Moon, M.H.; Xu, Y.; Giddings, J.C. Effect of viscosity on retention time and hydrodynamic lift forces in sedimentation/steric field-flow fractionation. Chem. Eng. Sci. **1996**, *51* (19), 4477–4488.
29. Schimpf, M.E.; Giddings, J.C. Characterization of thermal diffusion in polymer solutions by thermal field-flow fractionation: dependence on polymer and solvent parameters. J. Polym. Sci. Polym. Phys. **1989**, *27* (6), 1317–1332.
30. Gunderson, J.J.; Caldwell, K.D.; Giddings, J.C. Influence of temperature gradients on velocity profiles and separation parameters in thermal field-flow fractionation. Sep. Sci. Technol. **1984**, *19* (10), 667–683.

Received May 12, 2004
Accepted June 20, 2004
Manuscript 6409